

# Evaluation of oxidative response and tissular damage in rat lungs exposed to silica-coated gold nanoparticles under static magnetic fields

Soumaya Ferchichi<sup>1</sup>  
Hamdi Trabelsi<sup>1</sup>  
Inès Azzouz<sup>1</sup>  
Amel Hanini<sup>2</sup>  
Ahmed Rejeb<sup>3</sup>  
Olfa Tebourbi<sup>1</sup>  
Mohsen Sakly<sup>1</sup>  
Hafedh Abdelmelek<sup>1</sup>

<sup>1</sup>Laboratory of Integrative Physiology,  
Faculty Of Sciences of Bizerte,

<sup>2</sup>Laboratory of Vascular Pathology,  
Carthage University, Carthage

<sup>3</sup>Laboratory of Pathological Anatomy,  
National School of Veterinary  
Medicine of Sidi Thabet, Manouba  
Univeristy, Manouba, Tunisia

**Abstract:** The purpose of our study was the evaluation of toxicological effects of silica-coated gold nanoparticles (GNPs) and static magnetic fields (SMFs; 128 mT) exposure in rat lungs. Animals received a single injection of GNPs (1,100 µg/kg, 100 nm, intraperitoneally) and were exposed to SMFs, over 14 days (1 h/day). Results showed that GNPs treatment induced a hyperplasia of bronchus-associated lymphoid tissue. Fluorescence microscopy images showed that red fluorescence signal was detected in rat lungs after 2 weeks from the single injection of GNPs. Oxidative response study showed that GNPs exposure increased malondialdehyde level and decreased CuZn-superoxide dismutase, catalase, and glutathione peroxidase activities in rat lungs. Furthermore, the histopathological study showed that combined effects of GNPs and SMFs led to more tissular damages in rat lungs in comparison with GNPs-treated rats. Interestingly, intensity of red fluorescence signal was enhanced after exposure to SMFs indicating a higher accumulation of GNPs in rat lungs under magnetic environment. Moreover, rats coexposed to GNPs and SMFs showed an increased malondialdehyde level, a fall of CuZn-superoxide dismutase, catalase, and glutathione peroxidase activities in comparison with GNPs-treated group. Hence, SMFs exposure increased the accumulation of GNPs in rat lungs and led to more toxic effects of these nanocomplexes.

**Keywords:** malondialdehyde, catalase, superoxide dismutase, glutathione peroxidase, bronchus-associated lymphoid tissue, nanotoxicity, histopathological study

## Introduction

The rapid emergence of gold nanoparticles (GNPs) technology holds great promise for future biomedical applications. In fact, due to a high stability, ease of synthesis, and straightforward incorporation of functional groups for targeting bio-applications, GNPs have several applications in cancer treatment, bioimaging, gene, and protein delivery.<sup>1-3</sup>

However, despite their huge potential benefits in biomedical, environmental, and industrial applications, very little is known about the short- or long-term bioeffects in organisms. Reports show that GNPs can circulate in the body for a long time without being rejected by the body and the immune system.<sup>1</sup> All these behaviors are guided by the small size, shape, and surface charges. This is of concern because during synthesis and applications, GNPs of various sizes, shapes, and surface charges are generated that may be of health risk.<sup>3</sup>

A previous study suggested that GNPs can be used safely.<sup>4</sup> However, other data found that gold was toxic to the body, where it becomes soluble by cyanidation and can undergo oxidation.<sup>3</sup> Investigations revealed that GNPs are heavily taken up by kidneys and can also initiate eryptosis.<sup>5,6</sup> Physicochemical properties related to size,

Correspondence: Soumaya Ferchichi  
Laboratory of Physiologie Intégrée,  
Faculty of Sciences of Bizerte, Carthage  
University, Carthage, Carthage – 7021,  
Tunisia  
Fax +216 2 72 590 566  
Email ferchichi.soumaya@gmail.com



shape, and surface charge are key factors associated with gold complexes toxicity.

Previous studies showed that following injection of colloidal gold in mice, particles with size range from 10 to 50 nm were dispersed rapidly to all tissues especially in lungs, liver, kidneys, and spleen.<sup>1,7,8</sup> These investigations pointed to a size-dependent distribution and potential toxicity of GNPs.<sup>1,7,8</sup>

Moreover, the rising use of electronic equipment leads to concerns about the health bioeffect of electromagnetic fields.<sup>9</sup> Previous biochemical investigations have been performed in order to evaluate the bioeffects of static magnetic fields (SMFs) on the metabolism of animals and humans.<sup>10</sup> These studies concluded that SMFs induced disruption in carbohydrate, lipid, and protein metabolism.<sup>11–13</sup> Other data showed that SMFs are involved in reactive oxygen species production, such as superoxide anion in different cells and organs.<sup>14–16</sup>

SMFs can affect membrane structure and function and cause DNA damage.<sup>15,16</sup> Previous data have also reported that SMFs interact with divalent cations in rats such as zinc (Zn),<sup>17</sup> selenium (Se),<sup>18</sup> iron (Fe),<sup>19</sup> and cadmium (Cd).<sup>20</sup> The analysis of the literature showed that there were few data discussing the interaction between SMFs and GNPs as previously described by Shaw et al.<sup>21</sup>

The purpose of our study was to evaluate oxidative response and tissular damages in rat lungs exposed to GNPs under magnetic environment.

## Materials and methods

### Chemicals

Silica-gold stabilized nanoparticles were purchased from Nano-H-SAS (Saint Quentin Fallavier, France). The size distribution of silica-coated GNP is determined to be 102.70 nm (Figure 1). The study of spectral properties showed that GNPs

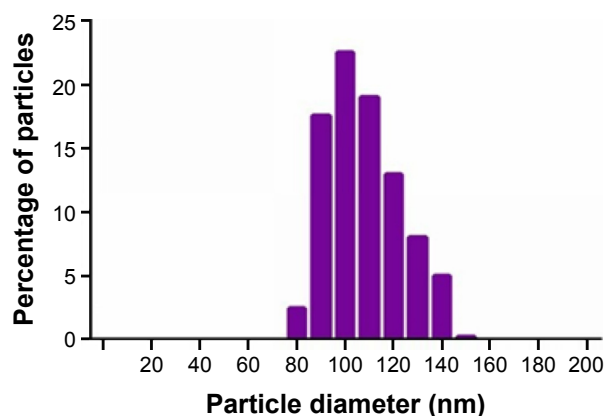


**Figure 1** Data related to size distribution of silica-coated gold nanoparticles.

used in our investigation have a wide excitation spectrum with a maximum absorbance detected at 525 nm.

By contrast, GNPs have a narrow emission spectrum. The highest emission was detected at 575 nm. All other chemicals used in the present study were of analytical grade and obtained from Sigma-Aldrich (St Louis, MO, USA) and Chemi-pharma (Le Bardo, Tunisia).

### Animals

In the present investigation, adult Wistar male rats (SIPHAT, Bin Arous, Tunisia) were used. Animal weights ranged from 180 to 200 g during the experimental period. Rats were randomly divided into four groups of six: control, GNPs-treated rats, SMF-exposed rats, and coexposed rats (GNPs + SMF). The animal well-being was considered during the study. Rats were housed at 25°C (12/12 hours light/dark cycle). Animals had free access to commercial mash and water. All our experimental protocols were approved by the Faculty of Sciences of Bizerte Ethics Committee. Animals were cared for, under the Tunisian code of practice for the Care and Use of Animals for Scientific Purposes.

### Treatment protocol by silica-coated GNPs and SMFs

The control group was intraperitoneally injected once with 0.10 mL of 0.90% saline solution. The GNPs-treated rats were injected once with silica-coated GNPs (1,100 µg/kg of body weight, intraperitoneally). The SMFs-exposed group was exposed for 1 h/day to the SMFs over 14 days. Coexposed rats (GNPs + SMF) were injected once with GNPs (1,100 µg/kg of body weight, intraperitoneally) exposed to SMFs (1 h/day) over 14 days.

### Exposure system

Lake Shore Electromagnets (Lake Shore Cryotronics, Inc, Westerville, OH, USA) are compact electromagnets suited for many applications, such as magnetic resonance demonstrations. For the present experiment, we have used an air gap of 15 cm. Water-cooled coils provide an excellent field for stability and uniformity when high power is required to achieve the maximum field capability for the electromagnet. We have an accurate pole alignment by precise construction of the air gap adjustment mechanism.<sup>22</sup> Intensity of SMF was measured and standardized over the total floor area of the Plexiglas cage at 128 mT. The cage is 20×10×20 cm. The two bobbins of the Lake Shore System were separated by 12 cm. Rats were placed at the

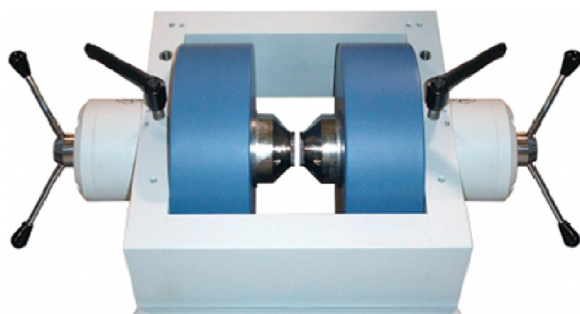


**Figure 2** Lake Shore electromagnets.

center of uniform field area (Figure 2). Uniformity of the SMF in the active exposure volume was  $\pm 0.2\%$  over 1 cm. The cage in the Lake Shore System contained two rats for each exposure.

## Histology and light microscopy

Lung fractions were fixed in buffered formalin. Fractions were blocked in paraffin and sections of  $\sim 5 \mu\text{m}$  were performed. These sections were stained with hematoxylin and eosin. The analysis of histopathological data was carried out by a semistatistical evaluation based on the frequency of structural changes. The following symbols were used: –, absence of structural changes; +, a rare structural change within a group; +++–, a structural change observed in almost all animals of a group; +++, a structural change found in all animals of a group.

## Fluorescence microscopy analysis

Lung fractions were fixed in formaldehyde. Fluorescence microscopy analysis was performed using a Leica DM-IRB Inverted fluorescence microscope (Leica Microsystems, Wetzlar, Germany). The used microscope is equipped with mercury arc lamp with an excitation wavelength of 540 nm and with a digital camera (CCD camera CoolSNAP™, Princeton Instruments, Trenton, NJ, USA). Fluorescence images were obtained with  $\times 40$  enlargement and an emission filter set at 620 nm. Image processing was carried out using Leica IM50 version 5.00 software (Leica Microsystems, Wetzlar, Germany).

## Tissue preparation

All groups were sacrificed and their lungs were harvested. Lungs were weighted, rinsed, and dried. Lungs were homogenized in buffer (tris[hydroxymethyl]aminomethane 10 mmol/L, ethylenediaminetetraacetic acid 1 mmol/L, phenylmethylsulfonyl fluoride 1 mmol/L; pH 7.4). The homogenates were centrifuged at  $600\times g$  for 10 minutes and centrifuged again at  $13,000\times g$  for 20 minutes at  $4^\circ\text{C}$  to have a postnuclear homogenate and postmitochondrial supernatant fractions.<sup>23</sup>

## Evaluation of oxidative response

Malondialdehyde (MDA) content was evaluated by thiobarbituric acid reactive substances.<sup>24</sup> The analysis of catalase (CAT) activity was performed by ultraviolet spectrophotometry.<sup>25</sup> The activity of glutathione peroxidase (GPx) was studied according to Gunzler et al.<sup>26</sup> Superoxide dismutase (SOD) activity was investigated based on the inhibition of the auto-oxidant of pyrogallol at 420 nm, according to the modified method published previously by Marklund and Marklund.<sup>27</sup>

## Statistical analysis

All our data were reported as mean  $\pm$  standard deviation and the level of significance was set at  $P < 0.05$ . GraphPad Prism version 6.00 for Windows (GraphPad Software Inc, La Jolla, CA, USA) was used to perform a one-way analysis of variance followed by Tukey's multiple comparisons test.

## Results

### Histopathological analysis

The analyses of lung sections of control rats and rats exposed to SMFs have not revealed any structural changes. However, hyperplasia of bronchus-associated lymphoid tissue was evident after GNPs treatment (1,100  $\mu\text{g/kg}$ , single injection, intraperitoneally) (Table 1, Figure 3). Interestingly, coexposure to GNPs (1,100  $\mu\text{g/kg}$ , intraperitoneally) and SMFs led to higher hyperplasia of bronchus-associated lymphoid tissue than GNPs-treated group. In addition, light microscopic

**Table 1** Histopathological findings in lungs of rats following gold nanoparticles treatment and/or static magnetic fields exposure

Histopathological findings	Control	SMF	GNPs	GNPs + SMF
Hyperplasia of bronchus-associated lymphoid tissue	–	–	–+	+++–
Granuloma	–	–	–	+++–
Alveolar compression	–	–	–+	+++–

**Notes:** –, absence of structural changes; +, a rare structural change within a group; +++–, a structural change observed in almost all animals of a group; +++, a structural change found in all animals of a group.

**Abbreviations:** GNPs, gold nanoparticles; SMF, static magnetic field.



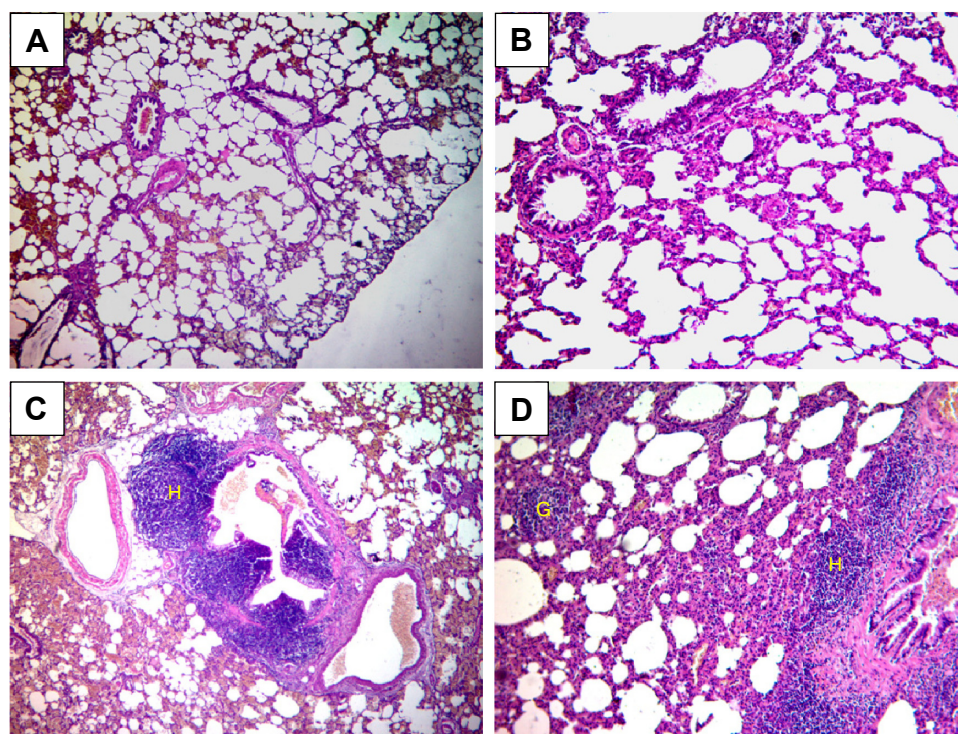


**Figure 3** Structural changes in rat lungs following exposure to GNPs and/or SMFs.

**Notes:** (A) Normal structure of lungs in control rats. (B) Normal structure of lungs in rats exposed to SMFs for 14 days. (C) Lung structure of GNPs-treated rats. (D) Lung structure of coexposed rats to GNPs and SMFs.  $\times 100$  magnification.

**Abbreviations:** G, granuloma; GNPs, gold nanoparticles; H, hyperplasia; SMFs, static magnetic fields.

examination showed the presence of granuloma and an alveolar compression after coexposure to GNPs and SMFs (Table 1, Figure 3).

## Fluorescence microscopy analysis

In control rats, images showed the absence of fluorescence signal (Figure 4A and B). Similar results were observed following SMFs exposure (Figure 4C and D). By contrast, fluorescence image processing revealed red fluorescence signal in lungs after GNPs treatment (Figure 4E and F). Importantly, coexposure to GNPs and SMFs increased fluorescence intensity compared to GNPs-treated rats (Figure 4G and H).

## Evaluation of oxidative response following GNPs treatment under SMFs

### MDA level

Exposure to SMFs led to an increase in MDA level ( $1.51 \pm 0.05$  nmol/mg protein vs  $1.08 \pm 0.06$  nmol/mg protein;  $P < 0.05$ ). In addition, GNPs treatment ( $1,100 \mu\text{g/kg}$ , intraperitoneally) increased MDA level ( $1.93 \pm 0.05$  nmol/mg protein vs  $1.08 \pm 0.06$  nmol/mg protein;  $P < 0.01$ ). Coexposure

to GNPs and SMFs led to a higher increase in MDA level compared with control rats ( $2.83 \pm 0.06$  nmol/mg protein vs  $1.08 \pm 0.05$  nmol/mg protein;  $P < 0.001$ ) (Figure 5). Interestingly, MDA level was higher in coexposed group to GNPs and SMFs compared to GNPs-treated rats ( $2.83 \pm 0.06$  nmol/mg protein vs  $1.93 \pm 0.05$  nmol/mg protein;  $P < 0.01$ ).

## Evaluation of antioxidant enzymes activities

Antioxidant enzymes assays showed that acute exposure to SMFs (128 mT, 1 h/day) induced a decrease in GPx ( $-56\%$ ), CAT ( $-15\%$ ), and CuZn-SOD ( $-80\%$ ) activities (Table 2). In addition, GNPs treatment ( $1,100 \mu\text{g/kg}$ , intraperitoneally) reduced the pulmonary activities of GPx ( $-48\%$ ) compared with control. The same treatment induced a depletion of CAT ( $-62\%$ ) and CuZn-SOD ( $-82\%$ ) activities compared to control. Furthermore, coexposure to SMFs and GNPs decreased GPx ( $-53\%$ ), CAT ( $-71\%$ ), and CuZn-SOD ( $-87\%$ ) in rat lungs (Table 2).

## Discussion

The aim of our study was to evaluate the effects of SMFs on silica-coated GNPs acute toxicity in rat lungs.

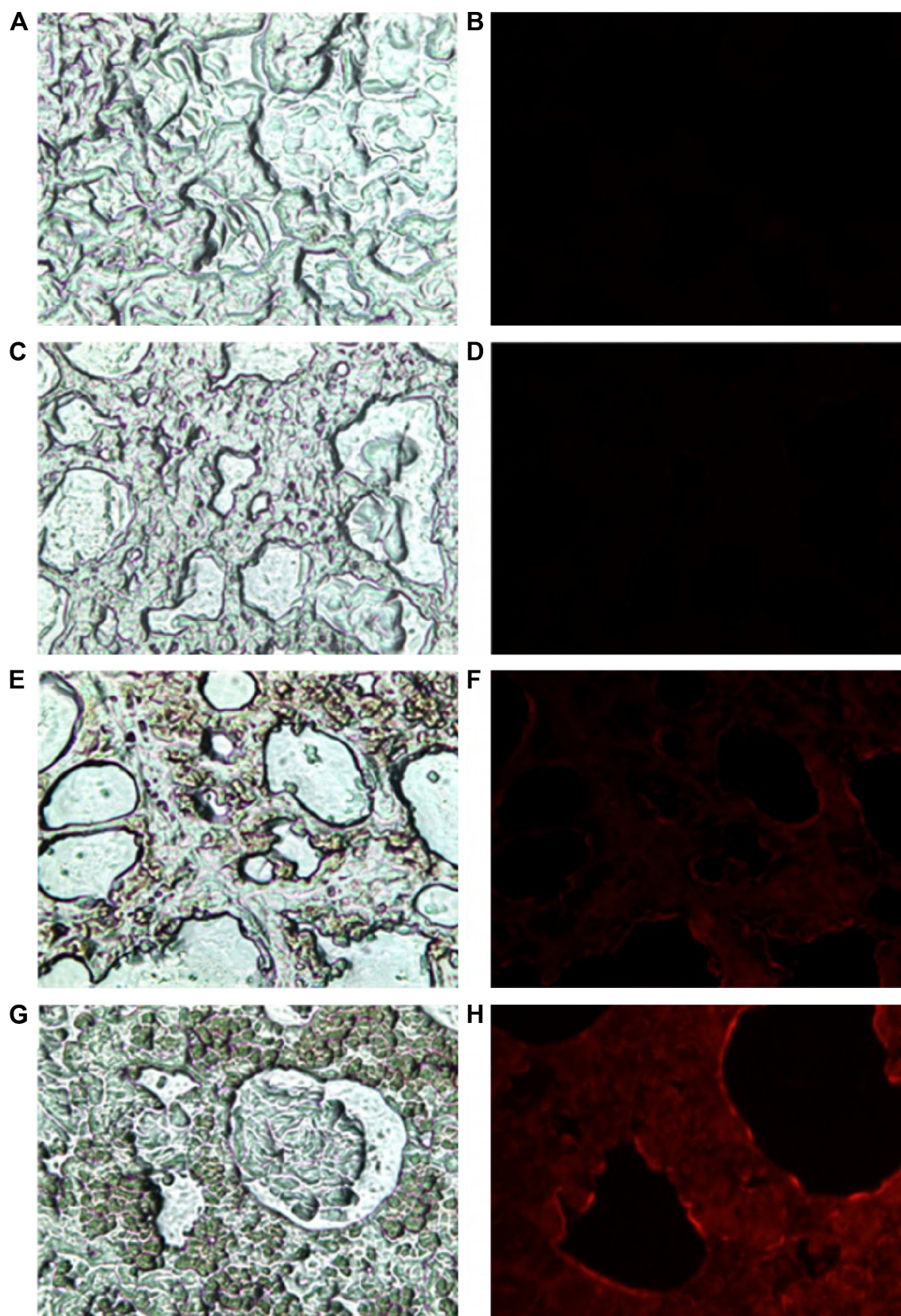


**Figure 4** Fluorescence microscopy images of lung fractions of rats exposed to gold nanoparticles and/or static magnetic fields.

**Notes:** Light microscopy (A) and fluorescence microscopy (B) of lung sections of control rats. Light microscopy (C) and fluorescence microscopy (D) of lung sections of SMF-exposed rats. Light microscopy (E) and fluorescence microscopy (F) of lung sections of GNPs-treated rats. Light microscopy (G) and fluorescence microscopy (H) of lung sections of coexposed rats to gold nanoparticles and static magnetic field.  $\times 100$  magnification.

**Abbreviations:** GNPs, gold nanoparticles; SMF, static magnetic field.



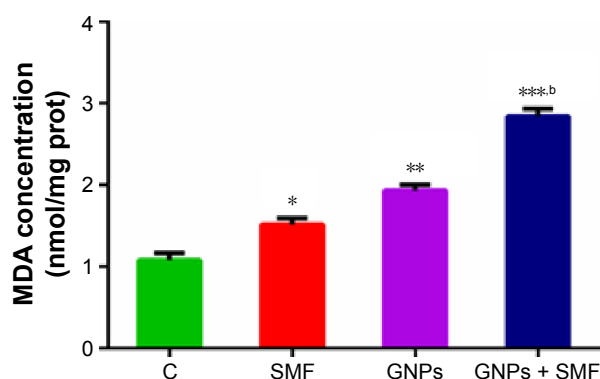


**Figure 5** Effects of gold nanoparticles and static magnetic field on pulmonary MDA level.

**Notes:** Results represent mean  $\pm$  SD of six animals per group. \* $P < 0.05$ ; \*\* $P < 0.01$ ; \*\*\* $P < 0.001$  compared with control rats. <sup>b</sup> $P < 0.01$  compared with GNPs-treated group. Results are in response to a one-way analysis of variance.

**Abbreviations:** C, control; GNPs, gold nanoparticles; MDA, malondialdehyde; prot, protein; SMFs, static magnetic fields; SD, standard deviation.

The investigation indicated that GNPs induced lung nanotoxicities in rats as previously demonstrated with other kinds of nanoparticles in lungs and different organs.<sup>28–30</sup> Light microscopy data showed the absence of tissular damages in lungs of control rats. Moreover, the exposure to SMFs failed to alter lungs architecture in rats. However, GNPs treatment induced mild epithelial hyperplasia, prominent inflammatory cells infiltrate, and enlarged airway cavities. Previously, similar data were reported by Terentyuk et al<sup>31</sup> and Schulz et al;<sup>32</sup> indicating that gold may induce inflammatory processes. Previously, Abdelhalim and Jarrar<sup>33</sup> showed that exposure to GNPs led to a focal inflammatory reactions represented by higher number of alveolar macrophages. The same investigation revealed an intracytoplasmatically located GNPs associated with granulocytes and alveolar type II hyperplasia.<sup>33</sup> Similarly, Hanini et al<sup>28</sup> reported that exposure to magnetic nanoparticles such as iron oxide nanoparticles led to lung damages

**Table 2** Effects of silica-coated gold nanoparticles and static magnetic fields exposure on antioxidant enzymes activities in lungs

Groups	GPx (U/mg prot)	CAT (U/mg prot)	CuZn-SOD (U/mg prot)
Control	4.71 $\pm$ 0.17	210.08 $\pm$ 1.56	636.30 $\pm$ 94.97
SMF	2.07 $\pm$ 0.03***	179.30 $\pm$ 6.92*	127.90 $\pm$ 5.50**
GNPs	2.46 $\pm$ 0.04***	81.30 $\pm$ 1.73***	117.10 $\pm$ 30**
GNPs + SMF	2.26 $\pm$ 0.06***	62.24 $\pm$ 7.12***	84.16 $\pm$ 4.16**

**Notes:** Results represent mean  $\pm$  SD of six animals per group. \* $P < 0.05$ ; \*\* $P < 0.01$ ; \*\*\* $P < 0.001$  compared with control rats. Results are in response to a one-way analysis of variance.

**Abbreviations:** CAT, catalase; CuZn-SOD, CuZn-superoxide dismutase; GNPs, gold nanoparticles; GPx, glutathione peroxidase; prot, protein; SMF, static magnetic field; SD, standard deviation.

and increased leukocytes number related to an inflammatory process in rat.

Optical properties of GNPs were associated with plasmonic phenomena. The plasmonic properties of GNPs could be useful for biomedical applications.<sup>3</sup> Interestingly, red fluorescence signal was detected in rat lungs following GNPs treatment. The superposition of light microscopy images and fluorescence images revealed a localized fluorescence in lung cells but not in alveoli. In fact, biodistribution studies revealed that GNPs are promptly translocated from the bloodstream into organs as lungs, liver, and spleen.<sup>34–36</sup> In addition, many investigations reported that following parenteral administration, GNPs were detected in blood, lungs, heart, liver, spleen, stomach, small intestine, and kidneys.<sup>37–40</sup>

Moreover, previous investigations showed that distribution of GNPs in tissue is size-dependent,<sup>34,35</sup> dose-dependent,<sup>36</sup> and surface charge-dependent.<sup>37,38</sup> Furthermore, James et al<sup>41</sup> examined the biodistribution of GNPs and demonstrated a high accumulation of GNPs in lung 4 hours, 14 days, 21 days, and 28 days following the single administration.

Previous data pointed that parenteral or oral administration of metals induces biosynthesis of metallothioneins (MTs).<sup>42,43</sup> Gold (Au) could generate gold–MTs (Au–MTs) complexes after being bound to cysteine residues in MTs as previously demonstrated by Ariyasu et al.<sup>43</sup>

Trabelsi et al<sup>44</sup> found that subacute exposure to cadmium ions “Cd<sup>2+</sup>” could lead to nanoparticle biosynthesis in different organs. This finding was explained by the ability of Cd to react with sulfur in MTs and/or with selenium (Se) in rat hepatocytes and nephrocytes.<sup>44</sup> By an analogical explanation, we suggest that gold could interact with lung elements and generate nanocomplexes. The present hypothesis will be demonstrated in future studies.

The nanotoxicity of GNPs could be modulated by different environmental parameters such as SMFs, which is widely used. Our investigation showed cotreatment with GNPs and SMFs (GNP + SMF) increased red fluorescence signal in lungs. This finding can be explained by a higher accumulation of GNPs in rat lungs under magnetic environment. Bae et al<sup>45</sup> showed that SMFs enhanced cellular uptake of magnetic nanoparticles and generate their aggregation. Histological findings demonstrated that nanoparticles uptake was higher under SMFs. Previous data showed that magnetic fields accelerate the sedimentation of magnetic nanoparticles on cell surface.<sup>46–48</sup>

The appearance of lymphocytic infiltrate in lung tissues can be explained by the effects of GNPs on oxidative response leading to reactive oxygen species generation.<sup>33</sup> Oxidative

response results showed that exposure to GNPs or coexposure to GNPs and SMFs led to a higher MDA levels. In fact, previous data reported by Chater et al<sup>49</sup> and Amara et al<sup>50</sup> found that SMFs increased MDA level and induced a depression of antioxidant enzymes in rat liver, kidneys, and testis. These findings were associated with an imbalance of the intracellular redox homeostasis. Furthermore, SMFs may alter mineral elements homeostasis, which are essential in antioxidant enzyme biosynthesis.<sup>49,50</sup> Alteration of trace element (Se, Zn) by SMFs may disrupt the activities of antioxidant enzymes.<sup>51</sup> In addition, SMFs could induce change in the conformational structure of antioxidant enzymes, which alter their activities. Moreover, GNPs caused oxidative stress and cytotoxicity effects by catalyzing nitric oxide production. Reactive oxygen species generation could be related to the proportionately high surface area of GNPs.<sup>52–55</sup>

Furthermore, gold effects in cells could be related to its interactions with divalent mineral such as calcium ( $\text{Ca}^{2+}$ ), zinc ( $\text{Zn}^{2+}$ ), copper ( $\text{Cu}^{2+}$ ), iron ( $\text{Fe}^{2+}$ ), and selenium ( $\text{Se}^{2+}$ ). The mechanism of gold toxicity can be explained by its interactions with the enzymatic systems of cells resulting from the substitution of these mineral elements ( $\text{Zn}^{2+}$ ,  $\text{Cu}^{2+}$ ,  $\text{Se}^{2+}$ ) in metalloenzymes.<sup>43</sup>

The present results showed the ability of gold to induce oxidative stress in lungs as evidenced by a high level of lipid peroxidation (MDA) following GNPs treatment. These data are in agreement with previous findings reported by Ferreira et al.<sup>56</sup>

The lung MDA level in rats treated with gold is associated with a decrease in SOD, CAT, and GPx tissues activities, indicating an imbalance of the intracellular redox homeostasis.

The disruption of CuZn-SOD activity could be explained by the substitution of Zn by Au in CuZn-SOD. de Paula et al<sup>57</sup> showed that gold can occupy the site of Zn and other divalent elements. The mechanism of substitution of divalent element by metals (platinum [Pt], palladium [Pd], Au) can explain the oxidative disruption and probably the lack of generation of CuZn-SOD molecules, leading to an inactive form of the enzyme (CuAu-SOD). GNPs increased lipid peroxidation under magnetic environment. In addition, the combined effects of GNPs and SMFs led to higher antioxidant enzymes activities depletion compared to GNPs-treated rats. This result can be correlated to a higher red fluorescence signal detected after coexposure to SMFs and/or GNPs compared to GNPs-treated group. Previously, Trabelsi et al<sup>29</sup> established a ratio correlating the number of CdS/CdSe nanoparticles to oxidative response. Based on our findings, a similar ratio can

be described correlating the number of GNPs or fluorescence intensity to oxidative response parameters.<sup>29</sup>

$$\text{NanoMet(X)OR} = \frac{\text{Intensity of red fluorescence signal (number of GNPs)}}{\text{Antioxidant marker}}$$

where NanoMet(X) refers to metallic nanoparticles and OR to oxidative response. The ratio increase is correlated to the increase of GNPs number associated with fluorescence and a decrease in antioxidant enzymes activities. SMFs increased the accumulation of GNPs in lungs and lead to more depletion of antioxidant enzymes activities. This result must be evaluated by fluorescence imagery methods based on red fluorescence intensity.

## Conclusion

Our investigation reported that silica-coated nanoparticles could induce tissular damages and oxidative stress in rat lungs. In addition, acute exposure to SMF reinforced oxidative stress, observed following GNPs treatment in rat lungs.

## Acknowledgments

The authors would like to thank Ms Olfa Ajlani (Ibn Sina Secondary School, Menzel Bourguiba, Bizerte), Mr Bechir Azibe (Faculté des Sciences de Bizerte), and Mr Hazem Ben Mabrouk (Institut Pasteur de Tunis, Belvedere, Tunisia) for their help.

## Disclosure

The authors report no conflicts of interest in this work.

## References

1. De Jong WH, Hagens WI, Krystek P, Burger Sips AJ, Geertsma RE. Particle size-dependent organ distribution of gold nanoparticles after intravenous administration. *Biomaterials*. 2008;29:1912–1919.
2. Chen PC, Mwakwari SC, Oyelere AK. Gold nanoparticles: from nanomedicine to nanosensing. *Nanotechnology Sci Appl*. 2008;1:45–66.
3. Murphey CJ, Gole A, Stone JW, et al. Gold nanoparticles in biology: beyond toxicity to cellular imaging. *Acc Chem Res*. 2008;41:1721–1730.
4. Graham GG, Whitehouse MW, Bushell GR. Aurocyanide, dicyanoaurate (I), a pharmacologically active metabolite of medicinal gold complexes. *Inflammopharmacology*. 2008;16:126–132.
5. Sopjani M, Föller M, Lang F. Gold stimulates  $\text{Ca}^{2+}$  entry into and subsequent suicidal death of erythrocytes. *Toxicology*. 2008;244:271–279.
6. Sereemasun A, Rojanathanes R, Wiwanitkit V. Effect of gold nanoparticle on renal cell: an implication for exposure risk. *Ren Fail*. 2008;30:323–325.
7. Chithrani BD, Chan WCW. Elucidating the mechanism of cellular uptake and removal of protein-coated gold nanoparticles of different sizes and shapes. *Nano Lett*. 2007;7:1542–1550.

8. Sonavane G, Tomoda K, Makino K. Biodistribution of colloidal gold nanoparticles after intravenous administration: effect of particle size. *Colloids Surf B Biointerfaces*. 2008;66:274–280.
9. Forgacs Z, Somosy Z, Kubinyi G, et al. Effects of whole-body 50 Hz magnetic field exposure on mouse Leydig cells. *Sci World J*. 2004; 4:83–90.
10. Kula B, Grzesik J, Wardas M, Kuska R, Goss M. Effect of magnetic field on the activity of hyaluronidase and D-glucuronidase and the level of hyaluronic acid and chondroitin sulfate in rat liver. *Ann Acad Med Sil*. 1991;24:77–81.
11. Kula B, Sobczak A, Grabowska-bochenek R, Piskorska D. Effect of electromagnetic field on serum biochemical parameters in steelworkers. *J Occup Health*. 1999;41:177–180.
12. Chernysheva ON. Status of the lipid phase of plasma membranes of the rat heart after repeated exposure to alternative magnetic field of 50 Hz frequency. *Kosm Biol Aviakosm Med*. 1990;24:30–31.
13. Gorczyńska E, Węgrzynowicz R. Glucose homeostasis in rats exposed to magnetic fields. *Invest Radiol*. 1991;26:1095–1100.
14. Lupke M, Rollwitz J, Simko M. Cell activating capacity of 50 Hz magnetic fields to release reactive oxygen intermediates in human umbilical cord blood-derived monocytes and in Mono Mac 6 cells. *Free Radic Res*. 2004;38:985–993.
15. Savitz DA. Overview of occupational exposure to electric and magnetic fields and cancer: advancements in exposure assessment. *Environ Health Perspect*. 1995;103:69–74.
16. Simko M, Droste S, Kriehuber R, Weiss DG. Stimulation of phagocytosis and free radical production in murine macrophages by 50 Hz electromagnetic field. *Eur J Cell Biol*. 2001;80:562–566.
17. Amara S, Abdelmelek H, Abidi R, Sakly M, Ben Rhouma K. Zinc prevents hematological and biochemical alterations induced by static magnetic field in rats. *Pharmacol Rep*. 2005;57:616–622.
18. Ghodbane S, Amara S, Garrel C, et al. Selenium supplementation ameliorates static magnetic field-induced disorders in antioxidant status in rat tissues. *Environ Toxicol Phar*. 2011;31:100–106.
19. Elferchichi M, Ammari M, Maaroufi K, Sakly M, Abdelmelek H. Effects of exposure to static magnetic field on motor skills and iron levels in plasma and brain of rats. *Brain Inj*. 2011;25:901–908.
20. Amara S, Abdelmelek H, Garrel C, et al. Influence of static magnetic field on cadmium toxicity: study of oxidative stress and DNA damage in rat tissues. *J Trace Elem Med Biol*. 2006;20:263–269.
21. Shaw J, Raja SO, Dasgupta AK. Modulation of cytotoxic and genotoxic effects of nanoparticles in cancer cells by external magnetic field. *Cancer Nanotechnol*. 2014;5(1):2.
22. Abdelmelek H, Molnar S, Servais S, et al. Skeletal muscle HSP72 and norepinephrine response to static magnetic field in rat. *J Neural Transm*. 2006;113:821–827.
23. Beytut E, Aksakal M. The effect of long-term supplemental dietary cadmium on lipid peroxidation and the antioxidant system in the liver and kidneys of rabbits. *Turk J Vet Anim Sci*. 2002;26:1055–1060.
24. Placer ZA, Cushman LL, Johnson BC. Estimation of product of lipid peroxidation (malonyl dialdehyde) in biochemical systems. *Anal Biochem*. 1966;16:359–364.
25. Beers RF Jr, Sizer IW. A spectrophotometric method for measuring the breakdown of hydrogen peroxide by catalase. *J Biol Chem*. 1952;195: 133–140.
26. Gunzler WA, Kremers H, Flohe L. An improved coupled test procedure for glutathione peroxidase (EC 1-11-1-9-) in blood. *Z Klin Chem Klin Biochem*. 1974;12:444–448.
27. Marklund S, Marklund G. Involvement of the superoxide anion radical in the autooxidation of pyrogallol and a convenient assay for superoxide dismutase. *Eur J Biochem*. 1974;47:469–474.
28. Hanini A, Schmitt A, Kacem K, Chau F, Ammar S, Gavard J. Evaluation of iron oxide nanoparticle biocompatibility. *Int J Nanomedicine*. 2011;6:787–794.
29. Trabelsi H, Azzouz I, Ferchichi S, Tebourbi O, Sakly M, Abdelmelek H. Nanotoxicological evaluation of oxidative responses in rat nephrocytes induced by cadmium. *Int J Nanomedicine*. 2013;8:3447–3453.
30. Azzouz I, Trabelsi H, Hanini A, et al. Interaction between nanoparticles generated by zinc chloride treatment and oxidative responses in rat liver. *Int J Nanomedicine*. 2014;9:223–229.
31. Terentyuk G, Maslyakova G, Suleymanova L, et al. Circulation and distribution of gold nanoparticles and induced alterations of tissue morphology at intravenous particle delivery. *J Biophotonics*. 2009;2:292–302.
32. Schulz M, Ma-Hock L, Brill S, et al. Investigation on the genotoxicity of different sizes of gold nanoparticles administered to the lungs of rats. *Mutat Res*. 2012;745:51–57.
33. Abdelhalim MA, Jarrar BM. Gold nanoparticles administration induced prominent inflammatory, central vein intima disruption, fatty change and Kupffer cells hyperplasia. *Lipids Health Dis*. 2011;10:133.
34. Balasubramanian SK, Jittiwat J, Manikandan J, Ong CN, Yu LE, Ong WY. Biodistribution of gold nanoparticles and gene expression changes in the liver and spleen after intravenous administration in rats. *Biomaterials*. 2010;31(8):2034–2042.
35. Cho WS, Cho M, Jeong J, et al. Size-dependent tissue kinetics of PEG-coated gold nanoparticles. *Toxicol Appl Pharmacol*. 2010;245: 116–123.
36. Lasagna-Reeves C, Gonzalez-Romero D, Barria MA, et al. Bioaccumulation and toxicity of gold nanoparticles after repeated administration in mice. *Biochem Biophys Res Commun*. 2010;393:649–655.
37. Hirn S, Semmler-Behnke M, Schleh C, et al. Particle size-dependent and surface charge-dependent biodistribution of gold nanoparticles after intravenous administration. *Eur J Pharm Biopharm*. 2011;77:407–416.
38. Morais T, Soares ME, Duarte JA, et al. Effect of surface coating on the biodistribution profile of gold nanoparticles in the rat. *Eur J Pharm Biopharm*. 2012;80:185–193.
39. Fraga S, Brandão A, Soares ME, et al. Short- and long-term distribution and toxicity of gold nanoparticles in the rat after a single-dose intravenous administration. *Nanomedicine*. 2014;10:1757–1766.
40. Hillyer JF, Albrecht RM. Correlative instrumental neutron activation analysis, light microscopy, transmission electron microscopy, and X-ray microanalysis for qualitative and quantitative detection of colloidal gold spheres in biological specimens. *Microsc Microanal*. 1999;4:481–490.
41. James WD, Hirsch LR, West JL, O'Neal PD, Payne JD. Application of INAA to the build-up and clearance of gold nanoshells in clinical studies in mice. *J Radioanal Nucl Chem*. 2007;271:455–459.
42. Shrivastava R, Kushwaha P, Bhutia YC, Flora S. Oxidative stress induced following exposure to silver and gold nanoparticles in mice. *Toxicol Ind Health*. Epub 2014 Dec 29.
43. Ariyasu S, Onoda A, Sakamoto R, Yamamura T. Conjugation of Au11 cluster with Cys-rich peptides containing the alpha-domain of metallothionein. *Dalton Trans*. 2009;21(19):3742–3747.
44. Trabelsi H, Azzouz I, Sakly M, Abdelmelek H. Subacute toxicity of cadmium on hepatocytes and nephrocytes in the rat could be considered as a green biosynthesis of nanoparticles. *Int J Nanomedicine*. 2013;8:1121–1128.
45. Bae JE, Huh MI, Ryu BK, et al. The effect of static magnetic fields on the aggregation and cytotoxicity of magnetic nanoparticles. *Biomaterials*. 2011;32:9401–9414.
46. Dejardin T, de la Fuente J, Pino P, et al. Influence of both a static field and penetratin on magnetic nanoparticle delivery into fibroblasts. *Nanomedicine*. 2011;6:1719–1731.
47. Smith CA, de la Fuente J, Pelaz B, Furlani EP, Mullin M, Berry CC. The effect of static magnetic fields and tat peptides on cellular and nuclear uptake of magnetic nanoparticles. *Biomaterials*. 2010;15: 4392–4400.
48. Chaudhary S, Smith CA, del Pino P, et al. Elucidating the function of penetratin and a static magnetic field in cellular uptake of magnetic nanoparticles. *Pharmaceuticals*. 2013;6:204–222.
49. Chater S, Abdelmelek H, Couton D, Joulin V, Sakly M, Ben Rhouma K. Sub-acute exposure to magnetic field induced apoptosis in thymus of female rats. *Pak J Med Sci*. 2005;21:292–297.
50. Amara S, Abdelmelek H, Garrel C, et al. Zinc supplementation ameliorates static magnetic field-induced oxidative stress in rat tissues. *Environ Toxicol Pharmacol*. 2007;23:193–197.



51. Agay D, Anderson RA, Sandre C, Bryden NA, Alonso A, Roussel AM, Chancerelle Y. Alterations of antioxidant trace elements (Zn, Se, Cu and related metallo-enzymes in plasma and tissues following burn injury in rats. *Burns*. 2005;31:366–371.
52. Grigg J, Tellabati A, Rhead S, et al. DNA damage of macrophages at an air–tissue interface induced by metal nanoparticles. *Nanotoxicology*. 2009;3:348–354.
53. Tedesco S, Doyle H, Blascoc J, Redmond G, Sheehana D. Oxidative stress and toxicity of gold nanoparticles in *Mytilus edulis*. *Aquat Toxicol*. 2010;100:178–186.
54. Senaratne RH, De Silva AD, Williams SJ, et al. 5'-Adenosinephosphosulphate reductase (CysH) protects *Mycobacterium tuberculosis* against free radicals during chronic infection phase in mice. *Mol Microbiol*. 2006;59:1744–1753.
55. Pan Y, Leifert A, Ruau D, et al. Gold nanoparticles of diameter 1.4 nm trigger necrosis by oxidative stress and mitochondrial damage. *Small*. 2009;5:2067–2076.
56. Ferreira GK, Cardoso E, Vuolo FS, et al. Gold nanoparticles alter parameters of oxidative stress and energy metabolism in organs of adult rats. *Biochem Cell Biol*. 2015;93(6):548–557.
57. de Paula QA, Mangrum JB, Farrell NP. Zinc finger proteins as templates for metal ion exchange: substitution effects on the C-finger of HIV nucleocapsid NCp7 using M(chelate) species (M=Pt, Pd, Au). *J Inorg Biochem*. 2009;103(10):1347–1354.

### International Journal of Nanomedicine

### Publish your work in this journal

The International Journal of Nanomedicine is an international, peer-reviewed journal focusing on the application of nanotechnology in diagnostics, therapeutics, and drug delivery systems throughout the biomedical field. This journal is indexed on PubMed Central, MedLine, CAS, SciSearch®, Current Contents®/Clinical Medicine,

Submit your manuscript here: <http://www.dovepress.com/international-journal-of-nanomedicine-journal>

Journal Citation Reports/Science Edition, EMBase, Scopus and the Elsevier Bibliographic databases. The manuscript management system is completely online and includes a very quick and fair peer-review system, which is all easy to use. Visit <http://www.dovepress.com/testimonials.php> to read real quotes from published authors.

Dovepress